American Journal of Engineering and Applied Sciences

Original Research Paper

Preparation of $LiCoMnO_4$ Assisted by Hydrothermal Approach and its Electrochemical Performance

[1]Meilin You, [1]Xingkang Huang, [1]Min Lin, [1]Qingsong Tong, [1]Xiuhua Li, [1]Ying Ruan and [2]Yong Yang

[1]Department of Chemistry, Fujian Normal University, Fuzhou, China
[2]State Key Laboratory for Physical Chemistry of Solid Surfaces and Department of Chemistry, College of Chemistry and Chemical Engineering, Xiamen University, Xiamen, China

Article history
Received: 26-09-2015
Revised: 14-11-2015
Accepted: 21-05-2016

Corresponding Author:
Xingkang Huang and
Qingsong Tong
Department of Chemistry, Fujian Normal University, Fuzhou, China

Email: xkhuang@126.com and qstong_3503@fjnu.edu.cn

Yong Yang,
State Key Laboratory for Physical Chemistry of Solid Surfaces and Department of Chemistry, Chemical Engineering, Xiamen University, Xiamen, China
Email: yyang@xmu.edu.cn

Abstract: $LiCoMnO_4$ materials have been synthesized via a hydrothermal approach followed by a post-annealing process. Pure phase of $LiCoMnO_4$ is unable to form under hydrothermal conditions; however, high quality of pure $LiCoMnO_4$ was achieved after annealing the hydrothermal products. The concentration of LiOH and the post-annealing temperature are the crucial factors to form $LiCoMnO_4$. Without post-annealing process, the highest contents of $LiCoMnO_4$ in the hydrothermal products are less than 50% (e.g., in the presence of 1.2-1.35 M LiOH); in contrast, in the cases of 1.35-1.4 M LiOH, almost pure phase of $LiCoMnO_4$ has been achieved successfully after annealing the hydrothermal precursors at 750°C. The as-prepared sample in the presence of 1.35 M LiOH, after annealed at 750°C, exhibits a capacity of 91.6 mAh g^{-1}.

Keywords: Lithium Manganese Oxide, 5 V Spinel, Lithium-Ion Battery, Cathode

Introduction

$LiCoMnO_4$ possesses a spinel structure similar to $LiMn_2O_4$ and a high potential of ca. 5.0 V versus lithium. Compared to another 5 V spinel, $LiNi_{0.5}Mn_{1.5}O_4$ which has been investigated extensively (Li *et al*., 2007; Santhanam and Rambabu, 2010; Yang *et al*., 2011; Zhong *et al*., 2011; Cabana *et al*., 2012; Mao *et al*., 2012; Liu *et al*., 2012), $LiCoMnO_4$ is relatively new material. $LiNi_{0.5}Mn_{1.5}O_4$ is usually charged to cutoff voltages of 4.9-5.0 V (Liu *et al*., 2012; Shin *et al*., 2012; Yi and Hu, 2007; Huang *et al*., 2011) while $LiCoMnO_4$ has to be charged to 5.3 V due to its two charging plateaus at 5.2 and 4.9 V (Kawai *et al*., 1999; 1998; Huang *et al*., 2012; Hu *et al*., 2013; 2014; Kuwata *et al*., 2014). The main obstacle to practice $LiCoMnO_4$ is the requirement of electrolytes tolerant to high voltage above 5.0 V. Recent development of electrolytes such as reducing the contents of impurities and exploring new electrolytes (Markevich *et al*., 2006; Abouimrane *et al*., 2009) and additives (Lee *et al*., 2007; Xu *et al*., 2012; Abouimrane *et al*., 2013), offers a new chance for the practical application of $LiCoMnO_4$ as cathode materials for lithium-ion batteries. $LiCoMnO_4$ has been synthesized usually by solid-state reactions. For example, a $LiCoMnO_4$ was obtained by heating the stoichiometric mixtures of dried Li_2CO_3, CoO and $MnCO_3$ (Kawai *et al*., 1998). Our group recently has prepared $LiCoMnO_4$ via a sol-gel method (Huang *et al*., 2012). However, the synthesis of $LiCoMnO_4$ by a hydrothermal method has not reported, to the best of our knowledge. In this study, we obtained $LiCoMnO_4$ via the hydrothermal approach and investigated the effects of post-annealing on the hydrothermal products.

Experimental

About 0.005 mol $MnSO_4 \cdot H_2O$ (≥99%), 0.005 mol $CoSO_4 \cdot 7H_2O$ (≥98.5%) and 0.0075 mol $(NH_4)_2S_2O_8$ were dissolved in 20 mL deionized water solution in a 100 mL Teflon container, where $LiOH \cdot H_2O$ (≥98%) dissolved in 30 mL deionized water was added

dropwise. The Teflon container was then transferred to a stainless steel autoclave, sealed and heated at 220°C for 22 h. The resulting precipitate was separated from the solvents by filtration and then washed with deionized water. The sample was obtained after drying at 120°C for 24 h. To obtain the optimized conditions to synthesize $LiCoMnO_4$, 0.9-1.5 M LiOH were employed, where the concentration was calculated based the 50 mL solution in total. The hydrothermal products were heat-treated at 550-750°C.

The as-prepared samples were examined by powder X-Ray Diffraction (XRD) analysis, performed using a PANalytical X'Pert diffractometer with Cu Kα radiation (Philips). The XRD results were analyzed using an X'pert HighScore and X'pert Plus to obtain the crystal parameters of the samples. Morphology observation was studied by Scanning Electron Microscopy (SEM) performed with a Zeiss LEO1530.

Electrode fabrication and coin cell assembly were carried out as described in our previous report (Huang *et al*., 2009). In brief, the active material was mixed with 10 wt% acetylene black and 10 wt% binder (PVDF) and then ground by ball milling. The cathode was obtained by pressing the mixture onto a piece of aluminum foil followed by drying in a vacuum oven at 120°C for 2 h. The coin cells were fabricated with the prepared cathode, lithium anode, Celgard 2400 polypropylene separator and 1 M LPF_6 in ethylene carbonate/dimethyl carbonate (1:1 v/v) electrolyte. Cell testing was carried out at a constant current density of 140 mA g^{-1} at 27°C using a Land battery test system (Wuhan, China).

Results and Discussion

Figure 1 shows the XRD patterns of hydrothermal products in the presence of various LiOH concentrations. At low LiOH concentration such as 0.9-1.1 M, the as-obtained samples consist of $LiMn_2O_4$, Co_3O_4 and Mn_3O_4. The peaks located at between 29 and 34° should belong to Co-doped Hausmannite, namely $Co_xMn_{3-x}O_4$. The XRD peaks of Co_3O_4 are significantly overlapped with those of $LiMn_2O_4$; however, the intensity of the peak at ca. 36.5° is greater than that at ca. 18.8° (Fig. 1a and 1b), which suggests the existence of Co_3O_4. When LiOH concentration is higher than 1.2 M, these peaks over 29-34° disappeared, accompanied by decrease of the peak at 36.5° (Fig. 1c). These suggest that the contents of the impurities of Co_3O_4 and $Co_xMn_{3-x}O_4$ decreased. When the concentration of LiOH increased to 1.8 M, the intensity of the peak at ca. 44.5° turned higher than that at ca. 36.5°, which suggests the formation of Li_2MnO_3. As a result, spinel $LiMn_2O_4$ phase could be synthesized when the LiOH concentrations were employed in the range of 1.2-1.35 M in our experimental conditions. It is also notable that the peaks of the as-prepared $LiMn_2O_4$ shifted significantly toward high 2θ angle, which is due to the doping of cobalt ions in the structure of $LiMn_2O_4$ (Huang *et al*., 2012).

However, due to the similar structure between $LiMn_2O_4$ and $LiCoMnO_4$, it is difficult to distinguish them from the XRD patterns. Therefore, we examined the electrochemical performances of these hydrothermal samples. As shown in Fig. 2, when LiOH concentration is 0.9 M, it only shows a plateau at ca. 3.8 V. The plateau of $LiCoMnO_4$ (above 4.2 V) started to develop with the increase of LiOH concentration. The capacity above 4.2 V realted to $LiCoMnO_4$ reached the highest value at the LiOH concentration of 0.5 M. Beyond 0.5 M LiOH employed, Li_2MnO_3 phase was developed; as shown in Fig. 2 (above), when 1.8 M LiOH employed, the obtained sample presents a typical charge/discharge curves of Li_2MnO_3, exhibiting a discharge curve without remarkable plateau (Huang *et al*., 2009; Yue *et al*., 2008). This agrees well with the XRD result that the sample obtained in the presence of 1.8 M LiOH is composed of Li_2MnO_3 phase (Fig. 1f). This sample delivered a capacity of 167.0 mAh g^{-1} at the current density of 140 mAh g^{-1}, which is, however, beyond the interest of this study on 5 V spinel materials.

We obtained almost pure phase of $LiNi_{0.5}Mn_{1.5}O_4$ by the hydrothermal method in our previous report (Huang *et al*., 2011). In contrast, the hydrothermal approach to obtain pure phase of $LiCoMnO_4$ are still unsuccessful at this stage, which is evidenced by the fact that the discharge capacities of the samples obtained in the presence of 1.2-1.3 M LiOH are 70-80 mAh g^{-1} with ca. 35 mAh g^{-1} located above 4.2V. There are still some impurities such as $LiMn_2O_4$ and Li_2MnO_3 in these hydrothermal products. We then decided to employ post-annealing to improve the phase content of $LiCoMnO_4$.

As shown in Fig. 3, annealing hydrothermal products at 550°C resulted in broad XRD peaks with low intensities, while the peaks turned narrower and stronger as the annealing temperature increases. However, it seems no apparent difference between the XRD patterns of the samples obtained from various LiOH concentrations (1.1-1.4 M). Therefore, we compared these patterns by analyzing the (110) peak positions at ca. 19° and the Full-Width-at-Half-Maximum (FWHM) of these peaks as shown in Table 1. The FWHM values decreases with the annealing temperatures and with the increase of LiOH concentrations employed during the hydrothermal

reaction. Actually, the particle sizes of samples increased with the annealing temperatures as shown in Fig. 4. The primary particle size of the as-synthesized hydrothermal precursor (at 1.35 M LiOH) is ca. 30 nm (Fig. 4a); after annealing at 550°C, some crystal particles developed (Fig. 4b). When annealing at 750°C, the obtained sample shows well-defined crystals in 80-150 nm size range (Fig. 4c). On the other hand, at the same annealing temperatures, the higher the LiOH concentration, the higher angle the peak at the (110) plane moves towards as shown in Table 1. The parameters *a* of such samples were also calculated by assuming the pure phase of $LiCoMnO_4$. Generally, the higher LiOH concentration favors the smaller *a* value. Figure 5 show charge/discharge curves of annealed samples from the precursor prepared in the presence of 1.1 M LiOH. As shown in Fig. 5a, the samples after annealing at 550°C delivered an initial capacity of 54.5 mAh g^{-1} at a current density of 140 mA g^{-1} and decayed to 45.2 mAh g^{-1} after 5 cycles. There are two voltage plateaus at ca. 4.5 and 3.7 V, corresponding to the electrochemical pairs of Co(IV)/Co(III) and Mn(IV)/Mn(III), respectively, accompanied with insertion of Li^+ into the tetragonal 8a sites in the spinel structure. When the precursor was annealed at 650°C, the resulting product delivered 79.3 mAh g^{-1} until the voltage cutoff of 3.0 V and decayed to 67.9 mAh g^{-1} at the fifth cycle. If the voltage cutoff decreased to 2.0 V, the higher capacity of 164.0 mAh g^{-1} was achieved with a new developed voltage plateau at ca. 2.5 V which is associated with Mn (IV) changed to Mn (III) accompanied with Li^+ entering the octahedral 16c sites in the spinel structure. When the annealing temperature increased to 750°C, the as-obtained sample exhibits an initial capacity of 71.4 mAh g^{-1} and no obvious degeneration within 10 cycles as shown in Fig. 5c.

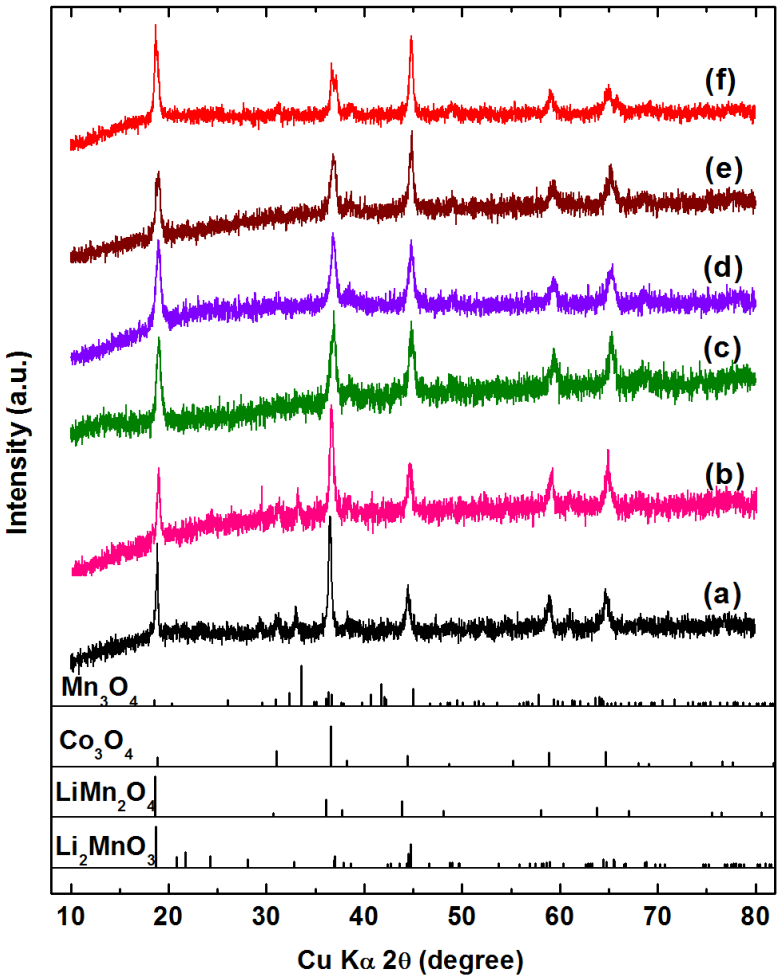

Fig. 1. XRD patterns of samples in the presence of (a) 0.1, (b) 0.3, (c) 0.4, (d) 0.5, (e) 0.55 and (f) 1.8 M LiOH at 220°C. The JCPDS numbers for Mn_3O_4, Co_3O_4, $LiMn_2O_4$ and Li_2MnO_3 are 80-382, 80-1536, 89-8321 and 84-1634, respectively

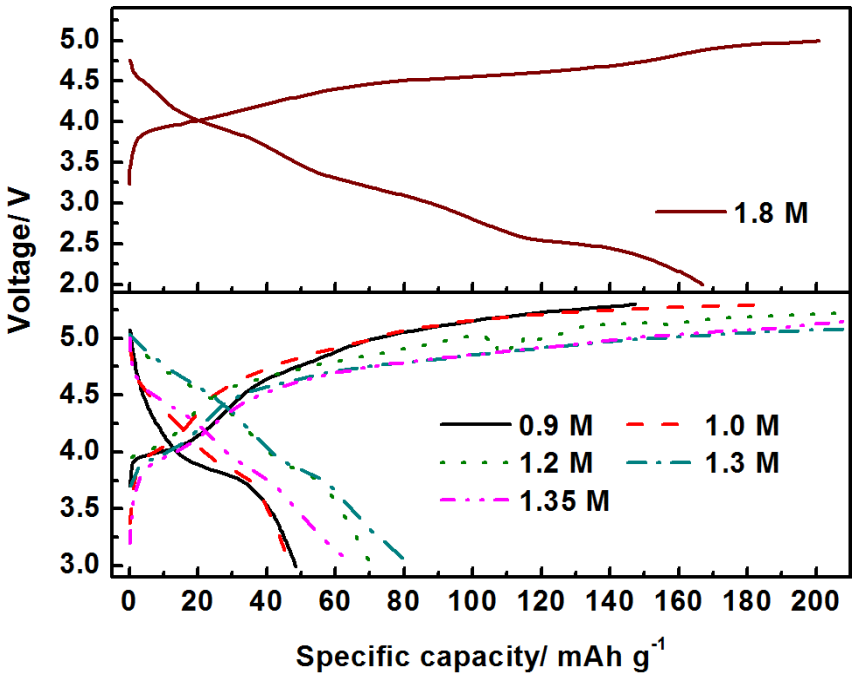

Fig. 2. Charge/discharge curves of hydrothermal products synthesized at various LiOH concentrations. The cutoff voltages were limited between 5.3 and 3.0 V except the case of 1.8 M LiOH which was limited between 4.8-2.0 V

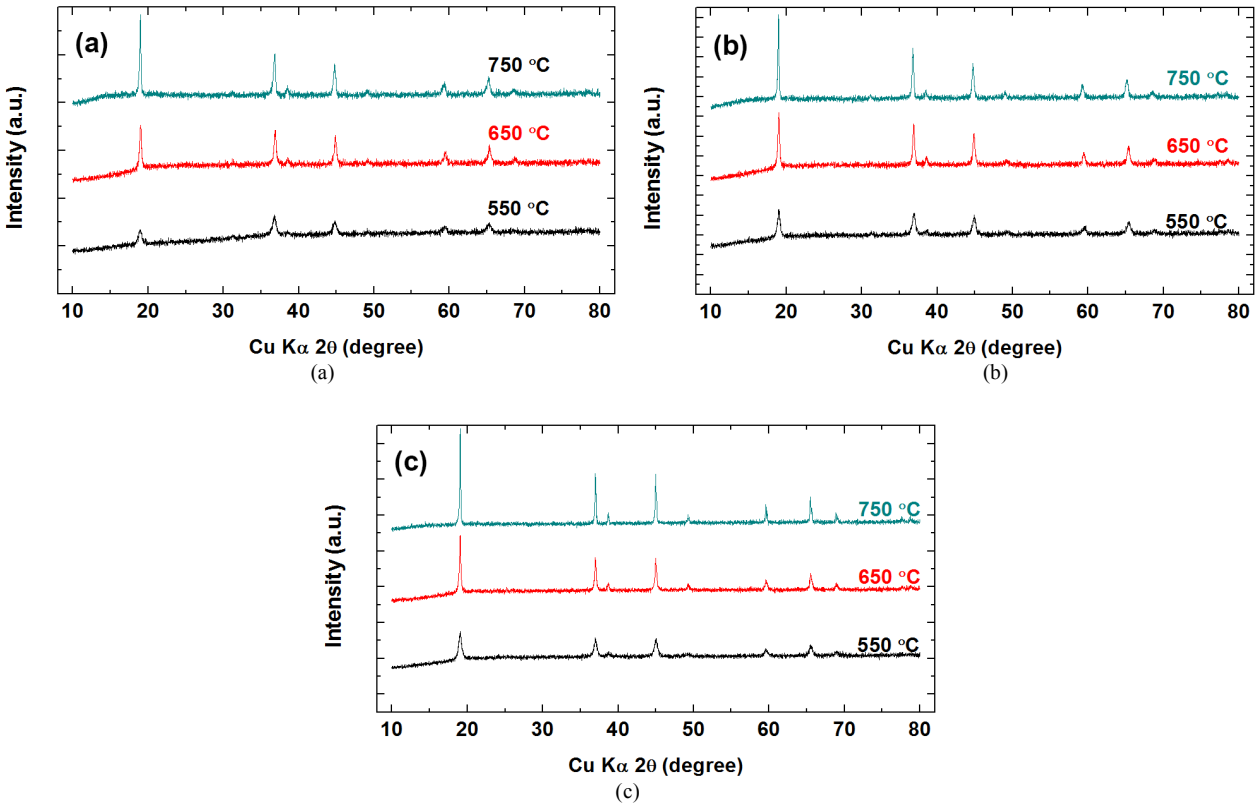

Fig. 3. Effect of post-annealing on the structures of hydrothermal precursors in the presence of (a) 1.1, (b) 1.2 and (c) 1.35 M LiOH

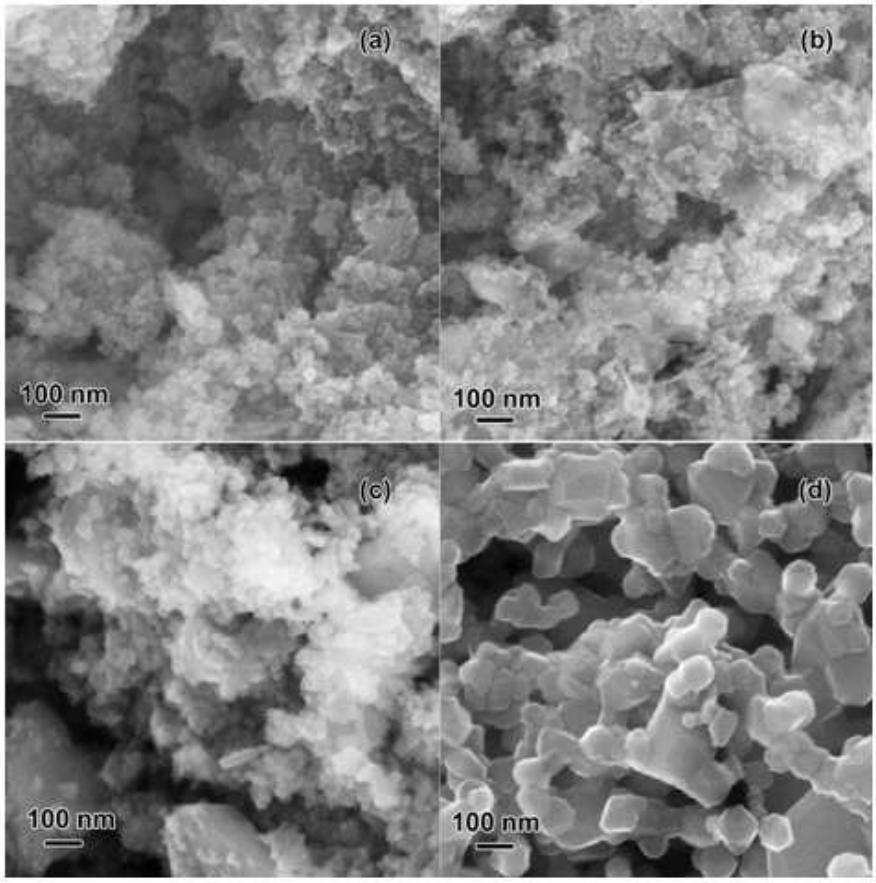

Fig. 4. SEM images of (a) the sample obtained in the presence of 1.35 M LiOH and its annealed samples at (b) 550, (c) 650 and (d) 750°C

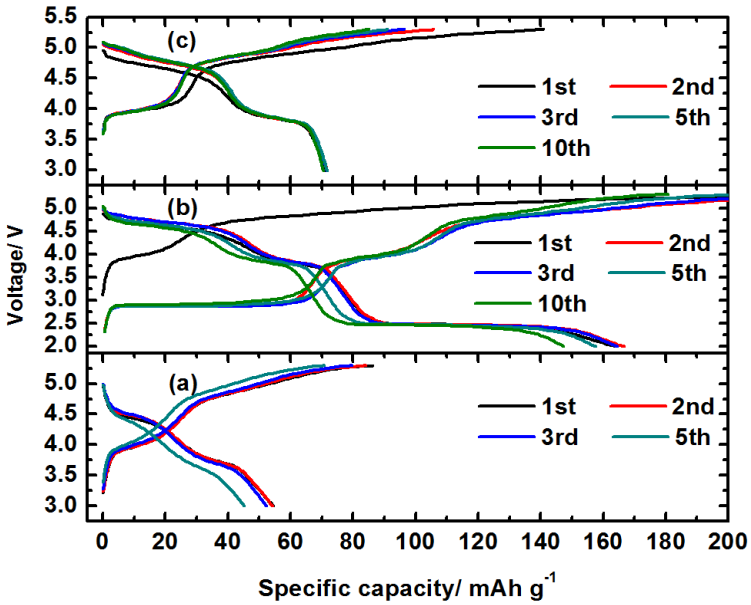

Fig. 5. Charge/discharge curves of samples obtained annealing the precursors in the presence of 1.2 M LiOH at (a) 550, 650 and 750°C

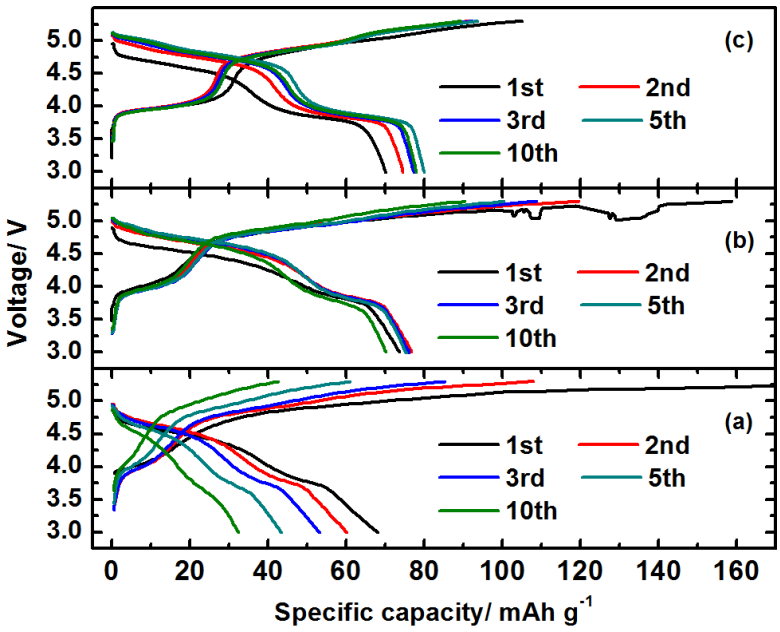

Fig. 6. Charge/discharge curves of samples obtained annealing the precursors in the presence of 1.1 M LiOH at (a) 550, 650 and 750°C

Table 1. XRD peak positions at the (110) plane of $LiCoMnO_4$ and crystal parameters of the samples by annealing the precursors obtained at various LiOH concentrations under the hydrothermal reaction

		XRD Peak @ (110)		
LiOH conc., M	Annealing temp., °C	Position, °	FWHM, °	Parameter *a*, Å
1.1	550	18.93	0.460	8.081(4)
1.1	650	18.98	0.264	8.0727(5)
1.1	750	18.95	0.188	8.090(1)
1.2	550	18.98	0.376	8.065(2)
1.2	650	18.98	0.252	8.073(2)
1.2	750	18.94	0.178	8.0705(9)
1.27	550	19.01	0.408	8.062(1)
1.27	650	19.01	0.282	8.059(2)
1.27	750	18.93	0.151	8.108(1)
1.35	550	19.03	0.415	8.0490(6)
1.35	650	19.04	0.223	8.048(1)
1.35	750	19.02	0.145	8.0527(5)
1.4	550	18.98	0.368	8.064(2)
1.4	650	19.04	0.201	8.0487(2)
1.4	750	19.04	0.113	8.0574(2)

When the precursor was prepared in the presence of 1.2 M LiOH, its annealed samples depict higher capacities at the 5 V-plateau zones (above 4.2 V), i.e., 35.3, 48.6 and 48.5 mAh g^{-1} for 550, 650 and 750°C, respectively (Fig. 6). On contrast, in the case of 1.35 M LiOH, the samples after annealing at 550, 650 and 750°C delivered discharge capacities of 52.2, 75.3 and 91.6 mAh g^{-1}, with 34.1, 61.8, 79.5 mAh g^{-1} located at above 4.2 V, corresponding to 65.3, 82.1 and 86.8% of their total capacities, respectively (Fig. 7). The discharge capacity of the sample obtained at 750°C is comparable to those reported in the literature on $LiCoMnO_4$ synthesized by a solid-state reaction (Kawai *et al*., 1998) or sol-gel method (Huang *et al*., 2012). Kawai *et al*. (1998) prepared a $LiCoMnO_4$ by the solid-state reaction, which delivered a discharge capacity of ca. 95 mAh g^{-1}. Huang *et al*. (2012) employed the sol-gel method to prepared a $LiCo_{1.09}Mn_{0.91}O_4$ exhibiting a capacity of 87.1 mAh g^{-1}.

When the employed LiOH concentration increased to 1.4 M, the as-obtained samples behaved like the case in the presence of 1.35 M LiOH (not shown here).

Beyond this concentration, e.g., at 1.5 M LiOH, rocksalt phase of Li_2MnO_3 was developed. As shown in Fig. 8, a shoulder peak at ca. 18.7° that belongs to Li_2MnO_3 appeared near the main peak at ca. 19.0° ascribed to $LiCoMnO_4$. The contents of Li_2MnO_3 in samples annealed from the precursor in the presence of 1.5 M LiOH are 22.8-26.5%, calculated by integrating the XRD peak area at 18.7° after separating it from the main peak at 19.0° (Fig. 8). The existence of Li_2MnO_3 in these samples is also supported by their discharge profiles as shown in Fig. 9. The voltage cutoffs were extended to 2.0 V to exhibit the discharge profile of Li_2MnO_3. The discharge capacity located at the oblique-line zone of 3.5-2.5 V was ascribed to the contribution of Li_2MnO_3 in the samples (Fig. 9). The unmarked voltage plateau is a characteristic of discharge process of Li_2MnO_3 materials (Robertson and Bruce, 2002; Yue *et al*., 2008; Huang *et al*., 2009). Note that extending the voltage cutoff to 2.0 V resulted in higher capacity (157.5, 168.3 and 121.2 mAh g^{-1} for samples annealed at 550, 650 and 750°C); however, the capacities decayed more quickly.

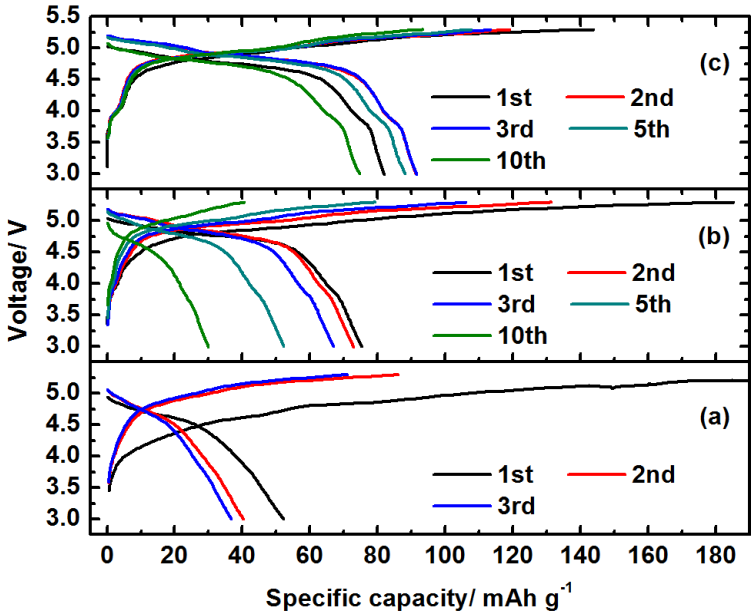

Fig. 7. Charge/discharge curves of samples obtained annealing the precursors in the presence of 1.35 M LiOH at (a) 550, 650 and 750°C

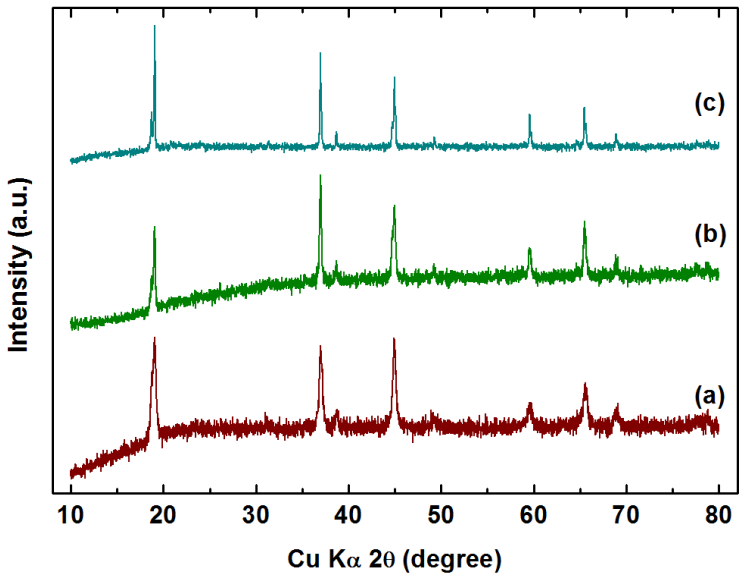

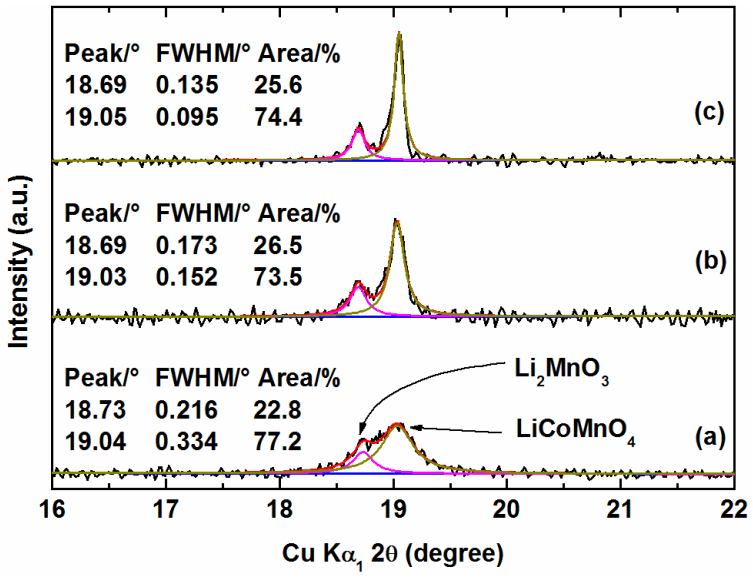

Fig. 8. XRD patterns of samples obtained in the presence of 1.5 M LiOH annealed at (a) 550, (b) 650 and (c) 750°C. The enlarged patterns between 18 and 22° were shown at the bottom, where peak fitting was performed after striping $K\alpha_2$

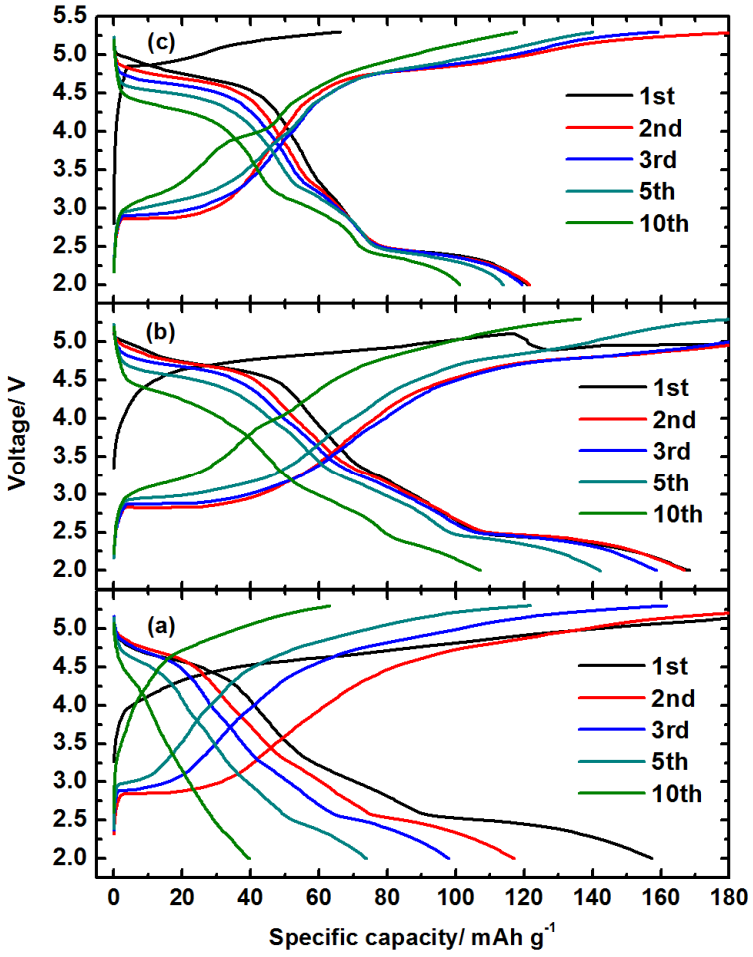

Fig. 9. Charge/discharge curves of samples obtained in the presence of 1.5 M LiOH annealed at (a) 550, (b) 650 and (c) 750°C

Finally we can conclude that the synthesis of $LiCoMnO_4$ is very sensitive to the concentration of LiOH employed during hydrothermal reaction. We also noticed that it is very sensitive to LiOH and NaOH during hydrothermal preparations of $LiNi_{0.5}Mn_{1.5}O_4$ (Huang *et al*., 2011) and γ-MnO_2 (Lv *et al*., 2009), respectively. Therefore, it is worthy of note that a desired hydrothermal product may be obtained only in a narrow range of alkaline concentration.

Conclusion

$LiCoMnO_4$ materials were synthesized via a hydrothermal approach followed by a post-annealing process. The concentration of LiOH significantly affects the hydrothermal precursors and the final annealed samples. At relatively low LiOH concentration (0.9-1.1 M), the as-prepared hydrothermal precursors consist of $LiMn_2O_4$ as a major phase with Co_3O_4 and Mn_3O_4 as impurity phases. 1.2-1.35 M LiOH is the suitable condition for the formation of spinel phases while too high concentration of LiOH such as 1.5 M results in the development of Li_2MnO_3.

However, without post-annealing process, the highest contents of $LiCoMnO_4$ in the hydrothermal products are still less than 50% (e.g., in the case of 1.2-1.35 M LiOH); in contrast, after annealing the hydrothermal precursors, the $LiCoMnO_4$ contents in the as-obtained samples improved significantly. The annealing temperature also highly influences the structures and electrochemical performance of the final samples. In general, a higher annealing temperature results in a better crystallinity of the final product. However, the effect of the annealing temperature on the $LiCoMnO_4$ content and electrochemical performance is cooperative with the LiOH concentration for its hydrothermal precursor. As a result, the optimized conditions are 1.35-1.4 M LiOH for hydrothermal precursors and 750°C for the post-annealing temperature. For example, the as-prepared sample in the presence of 1.35 M LiOH, after annealed at 750°C, delivered a capacity of 91.6 mAh g^{-1} with 79.5 mAh g^{-1} located at above 4.2 V.

Funding Information

This work is supported by Science and Technology Project from the Educational Commission of Fujian Province, China (Grant no. JA10072), Grant for Distinguish Young Scholar in Universities of Fujian Province, China (no. JA11040) and Science Foundation of Fujian Province, China (Grant no. 2011J05021). Y.Y. gratefully acknowledges the financial support from the National Basic Research Program of China (973 Program) (Grant no. 2007CB209702) and the National Natural Science Foundation of China Grants (Nos. 20473060, 29925310 and 20021002). Y.R. thanks Creative Experiments Project for Undergraduate Students of Fujian Province, China (no. Fjnu2011-022).

Author's Contributions

X.K.H., Q.S.T. and Y.Y conceived the idea. X.K.H. designed the experiments. M.L.Y., M.L., Y.R. carried out the material synthesis and characterization. X.K.H., Q.S.T. and Y.Y supervised all experimental design, tests and analyses and co-wrote the paper. All authors discussed the results and commented on the manuscript.

Ethics

These authors have no ethical issues that may arise after the publication of this manuscript.

References

Abouimrane, A., I. Belharouak and K. Amine, 2009. Sulfone-based electrolytes for high-voltage Li-ion batteries. Electrochem. Commun., 11: 1073-1076. DOI: 10.1016/j.elecom.2009.03.020

Abouimrane, A., S.A. Odom, H. Tavassol, M.V. Schulmerich and H.M. Wu *et al*., 2013. 3-Hexylthiophene as a stabilizing additive for high voltage cathodes in lithium-ion batteries. J. Electrochem. Soc., 160: A268-A271. DOI: 10.1149/2.039302jes

Cabana, J., M. Casas-Cabanas, F.O. Omenya, N.A. Chernova and D. Zeng *et al*., 2012. Composition-structure relationships in the Li-ion battery electrode material $LiNi_{0.5}Mn_{1.5}O_4$. Chem. Mater., 24: 2952-2964. DOI: 10.1021/cm301148d

Hu, M., Y. Tian, L. Su, J. Wei and Z. Zhou, 2013. Preparation and Ni-doping effect of nanosized truncated octahedral $LiCoMnO_4$ as cathode materials for 5 V li-ion batteries. ACS Applied Mater Interfaces, 5: 12185-12189. DOI: 10.1021/am404250k

Hu, M., Y. Tian, J.P. Wei, D.G. Wang and Z. Zhou, 2014. Porous hollow $LiCoMnO_4$ microspheres as cathode materials for 5 V lithium ion batteries. J. Power Sources, 247: 794-798. DOI: 10.1016/j.jpowsour.2013.09.038

Huang, X.K., M. Lin, Q.S. Tong, X.H. Li and Y. Ruan *et al*., 2012. Synthesis of LiCoMnO4 via a sol-gel method and its application in high power $LiCoMnO_4/Li_4Ti_5O_{12}$ lithium-ion batteries. J. Power Sources, 202: 352-356. DOI: 10.1016/j.jpowsour.2011.11.028

Huang, X.K., Q.S. Zhang, H.T. Chang, J.L. Gan and H.J. Yue *et al*., 2009. Hydrothermal synthesis of nanosized $LiMnO_2$-Li_2MnO_3 compounds and their electrochemical performances. J. Electrochem. Soc., 156: A162-A168. DOI: 10.1149/1.3054397

Huang, X.K., Q.S. Zhang, J.L. Gan, H.T. Chang and Y. Yang, 2011. Hydrothermal synthesis of a nanosized $LiNi_{0.5}Mn_{1.5}O_4$ cathode material for high power lithium-ion batteries. J. Electrochem. Soc., 158: A139-A145. DOI: 10.1149/1.3521292

Kawai, H., M. Nagata, H. Kageyama, H. Tukamoto and A.R. West, 1999. 5 V lithium cathodes based on spinel solid solutions $Li_2Co_{1+X}Mn_{3-X}O_8$:-1 <= X <= 1. Electrochim. Acta, 45: 315-327. DOI: 10.1016/S0013-4686(99)00213-3

Kawai, H., M. Nagata, H. Tukamoto and A.R. West, 1998. A new lithium cathode $LiCoMnO_4$: Toward practical 5 V lithium batteries. Electroche. Solid State Lett., 1: 212-214. DOI: 10.1149/1.1390688

Kuwata, N., S. Kudo, Y. Matsuda and J. Kawamura, 2014. Fabrication of thin-film lithium batteries with 5-V-class $LiCoMnO_4$ cathodes. Solid State Ion., 262: 165-169. DOI: 10.1016/j.ssi.2013.09.054

Lee, H., S. Choi, S. Choi, H.J. Kim and Y. Choi *et al*., 2007. SEI layer-forming additives for $LiNi_{0.5}Mn_{1.5}O_4$/graphite 5 VLi-ion batteries. Electrochem. Commun., 9: 801-806. DOI: 10.1016/j.elecom.2006.11.008

Li, D.C., A. Ito, K. Kobayakawa, H. Noguchi and Y. Sato, 2007. Electrochemical characteristics of $LiNi_{0.5}Mn_{1.5}O_4$ prepared by spray drying and post-annealing. Electrochim. Acta, 52: 1919-1924. DOI: 10.1016/j.electacta.2006.07.056

Liu, D., J. Hamel-Paquet, J. Trottier, F. Barray and V. Gariepy *et al*., 2012. Synthesis of pure phase disordered $LiMn_{1.45}Cr_{0.1}Ni_{0.45}O_4$ by a post-annealing method. J. Power Sources, 217: 400-406. DOI: 10.1016/j.jpowsour.2012.06.063

Lv, D., X. Huang, H. Yue and Y. Yang, 2009. Sodium-ion-assisted hydrothermal synthesis of γ-MnO_2 and its electrochemical performance. J. Electrochem. Soc., 156: A911-A911. DOI: 10.1149/1.3206586

Mao, J., K.H. Dai and Y.C. Zhai, 2012. Electrochemical studies of spinel $LiNi_{0.5}Mn_{1.5}O_4$ cathodes with different particle morphologies. Electrochim. Acta, 63: 381-390. DOI: 10.1016/j.electacta.2011.12.129

Markevich, E., V. Baranchugov and D. Aurbach, 2006. On the possibility of using ionic liquids as electrolyte solutions for rechargeable 5 V Li ion batteries. Electrochem. Commun., 8: 1331-1334. DOI: 10.1016/j.elecom.2006.06.002

Robertson, A.D. and P.G. Bruce, 2002. The origin of electrochemical activity in Li_2MnO_3. Chem. Commun. (Camb), 7: 2790-2791. DOI: 10.1039/b207945c

Santhanam, R. and B. Rambabu, 2010. Research progress in high voltage spinel $LiNi_{0.5}Mn_{1.5}O_4$ material. J. Power Sources, 195: 5442-5451. DOI: 10.1016/j.jpowsour.2010.03.067

Shin, D.W., C.A. Bridges, A. Huq, M.P. Paranthaman and A. Manthiram, 2012. Role of cation ordering and surface segregation in high-voltage spinel $LiMn_{1.5}Ni_{0.5-x}M_xO_4$ (M = Cr, Fe and Ga) cathodes for lithium-ion batteries. Chem. Mater., 24: 3720-3731. DOI: 10.1021/cm301844w

Xu, M.Q., Y.L. Liu, B. Li, W.S. Li and X.P. Li *et al*., 2012. Tris (pentafluorophenyl) phosphine: An electrolyte additive for high voltage Li-ion batteries. Electrochem. Commun., 18: 123-126. DOI: 10.1016/j.elecom.2012.02.037

Yang, T.Y., N.Q. Zhang, Y. Lang and K.N. Sun, 2011. Enhanced rate performance of carbon-coated $LiNi_{0.5}Mn_{1.5}O_4$ cathode material for lithium ion batteries. Electrochim. Acta, 56: 4058-4064. DOI: 10.1016/j.electacta.2010.12.109

Yi, T.F. and X.G. Hu, 2007. Preparation and characterization of sub-micro $LiNi_{0.5-x}Mn_{1.5+x}O_4$ for 5V cathode materials synthesized by an ultrasonic-assisted co-precipitation method. J. Power Sources, 167: 185-191. DOI: 10.1016/j.jpowsour.2007.02.003

Yue, H., X. Huang, D. Lv and Y. Yang, 2008. Hydrothermal synthesis and electrochemical performance of $Li_{1.59}H_{0.41}MnO_3$ as a cathode material for lithium-ion battery. Electrochem. Solid-State Lett., 11: A163-A163. DOI: 10.1149/1.2955862

Zhong, G.B., Y.Y. Wang, Z.C. Zhang and C.H. Chen, 2011. Effects of Al substitution for Ni and Mn on the electrochemical properties of $LiNi_{0.5}Mn_{1.5}O_4$. Electrochim. Acta, 56: 6554-6561. DOI: 10.1016/j.electacta.2011.03.093